A BINARY LIQUID MIXTURE OF BIOETHANOL-WATER AND BIODIESEL-WATER AS FUEL FOR NSDC-L│NSDC│NSDC-L DIRECT ETHANOL-SOLID OXIDE FUEL CELL

Fitria Rahmawati[1, ✉], Arum Putri Parameswari[1]

Abstract. This research studies the possibility on using a binary liquid mixture of bioethanol-water and biodiesel-water as fuel for a NSDC-L│NSDC│NSDC-L single fuel cell. The ratio of bioethanol-water was 70:30, as well as the ratio of biodiesel-water. The fuel vapor flowed into the fuel cell system under the temperatures of 673, 773 and 873 K with a flow rate of 1–1.5 ml·min⁻¹. The highest power densities were found at 673 K which are 2.984 and 1.838 mW·cm⁻² for bioethanol-water and biodiesel-water, respectively. It is a promising result for a single fuel cell test with a very low rate of liquid fuel flow. Meanwhile, open circuit voltage (OCV) of the single fuel cell with bioethanol-water fuel is 1.439 V which is close to the theoretical OCV. However, OCV of the single fuel cell with biodiesel-water as fuel is 0.710 V which is lower than the theoretical OCV. Cell polarization seems still being the problem causing voltage loss during single fuel cell test.

Keywords: binary liquid mixture, fuel, solid oxide fuel cell, NSDC.

1. Introduction

Biofuel is a renewable fuel that is usually produced from fermented cellulose and starch, mostly extracted from sugarcane, wheat, and corn [1]. It is frequently used as additive for petroleum or diesel in a definite ratio [2]. Combustion of biofuels, such as bioethanol or biodiesel by combustion engine leads to some pollutant side products such as CO_2, CO, NO_x, and SO_x [3]. On the other hand, fuel cell as an electrochemical cell could transform the chemical energy of fuel into energy with less pollutant gases. Ethanol has been used as fuel in a direct ethanol fuel cell (DEFC), a fuel cell technology that adopts proton electrolyte membrane fuel cell (PEMFC), with a polymer

membrane as electrolyte [4]. The DEFC can operate without gas reforming step even under low operational temperature. However, the performance of DEFC will decrease if CO gas is produced and blocks the active electrodes. DEFC is also very sensitive to the change of temperature and humidity [5]. Meanwhile, direct ethanol-solid oxide fuel cell (DE-SOFC), a developed solid oxide fuel cell (SOFC), is a fuel cell technology with liquid ethanol as fuel. Low-temperature SOFCs which operate at 573–873 K are known as very suitable for direct biofuels application, since most biofuels can thermally crack into H_2 and CO_2, in which H_2 production may support fuel cell performance. In DE-SOFC, the ethanol fuel is changed to gas, whether through an external or internal reforming gas [6]. In an external reforming, liquid fuel vaporizes in an external high-temperature system. The vapor then mixes with water vapor before entering the fuel cell system. Meanwhile, in an internal direct reforming system, the liquid fuel vaporizes and mixes with water vapor in an internal fuel cell system, in which the fuel and water vaporize in different evaporators [7]. The internal-direct reforming system is now investigated and applied more due to its simple design and efficiency [8]. However, fuel and water are evaporated in different evaporators. A study about mix fuel-water evaporation in a single evaporator system to flows into fuel cell system has not been investigated yet.

DE-SOFC usually uses yttria stabilized-zirconia (YSZ), as electrolyte [9], or a composite of sodium carbonate-samarium doped ceria (NSDC) [10, 11]. DE-SOFC with YSZ electrolyte and an internal gas reforming system produces an energy density of 200 mW·cm⁻² at 1133 K [7]. However, handicap for SOFC with hydrocarbon fuel is the carbon deposition on anode compartment produced by side reaction [12, 13], especially when Ni-YSZ is used as anode. Ni-YSZ has good catalytic activity for C=H bond breaking. The deposited carbon can block the porous anode and increases diffusion resistance of fuel gas allowing cell performance reduction [14]. Some researchers have added some oxidizing agents such as H_2O, CO_2, or O_2 to reform

[1] Research Group of Solid State Chemistry & Catalysis,
Chemistry Department, Sebelas Maret University,
Jl. Ir. Sutami 36 A Kentingan Surakarta 57126, Indonesia
✉ fitria@mipa.uns.ac.id

the hydrocarbon fuel internally, and the method was called as direct internal reforming (DIR) [15, 16].

In accordance with other results it was found that ceria-based electrolyte supported onto Ni-YSZ anode can efficiently convert fuel into hydrogen by electrochemically generated steam. The fuel cell is more durable compared to anode without ceria-based electrolyte, due to carbon deposit formation within the first 5 h of fuel cell operation. Ceria based electrolyte can promote steam reforming reaction of ethanol. It confirms the feasibility of ceria-based electrolyte for internal reforming of biofuels SOFC [17]. The addition of cerium oxide or ceria with copper (Cu) to Ni-YSZ anode also can increase the carbon resistance and the service life of the direct methane solid oxide fuel cell [18]. Direct ethanol-solid oxide fuel cell, DE-SOFC with NSDC electrolyte produces 148 mW·cm^{-2} at 853 K [10], in which ethanol was reformed externally. Cerium oxide provides higher ionic conductivity at low to intermediate temperature;

therefore, the fuel cell shows comparable energy density even under lower operational temperature. In addition, the presence of alkali carbonate shows ability to inhibit reduction reaction of Ce (IV) to Ce(III) that can reduce fast the fuel cell performance. NSDC is also reliable for low-temperature SOFC, because of its high ionic conductivity at low temperatures of 673–873 K [19].

In this research, the fuels were binary liquid mixture of bioethanol-water and biodiesel-water at 70:30 of fuel-water composition. The binary liquid mixture was evaporated simultaneously in an evaporator, and the vapor flowed into the anodic compartment at a high operational temperature of 673, 773, and 873 K. The oxidant was oxygen of the air that was directly fed to cathode compartment. It is named as internal direct reforming with a scheme shown in Fig. 1a. In the internal direct reforming the fuel and steam flow into anodic compartment, meanwhile, in internal indirect reforming the fuel and steam flow into an internal reformer, as shown in Fig. 1b.
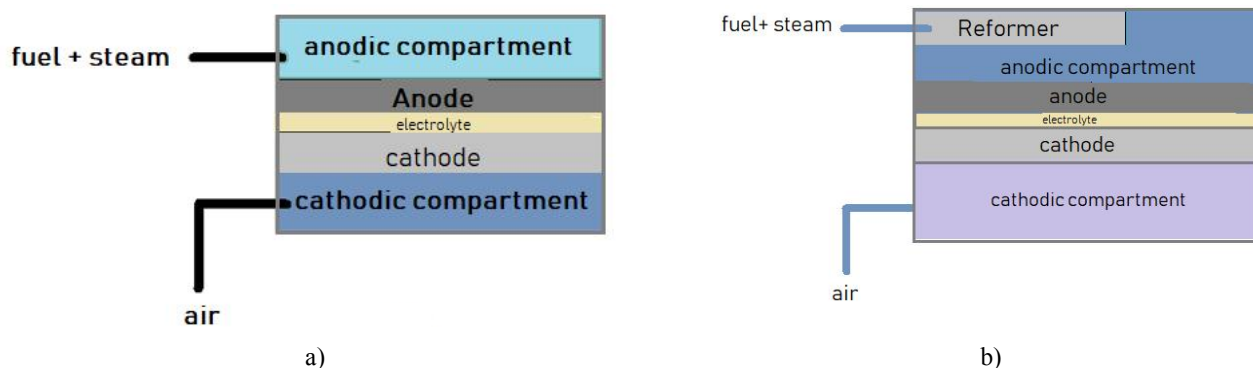

Fig. 1. Scheme of internal direct (a) and indirect (b) reforming

2. Experimental

2.1. Synthesis of Functional Materials

Samarium doped-ceria, $Ce_{0.8}Sm_{0.2}O_{1.9}$ (SDC), was synthesized from cerium nitrate hexahydrate $(Ce(NO_3)_3·6H_2O$ and samarium nitrate hexahydrate $(Sm(NO_3)_3·6H_2O)$ by sol-gel method. A stoichiometric amount of reactants was dissolved in 100 ml of water. A small amount of citric acid and polyethylene glycol (PEG) were added gradually into the mixture and the mixture was heated at 323 K under stirring. The PEG addition was conducted until a transparent yellow gel formed. The viscous gel was then heated to 673 K to form a yellow powder. The yellow powder was then calcined at 1073 K for 10 h.

Meanwhile, composite of sodium carbonate-SDC (NSDC) was prepared by co-precipitation method based on the previous publication [20]. The synthesis was

conducted by dissolving $Ce(NO_3)_3·6H_2O$ (99.99%) and $Sm (NO_3)_3·6H_2O$ (99.9%) in demineralized water with the ratio of $Ce^{3+} : Sm^{3+} = 4:1$ to produce a 100 ml reaction solution. An anhydrous $NaCO_3$ powder was dissolved in deionized water to produce a 200 ml of 1.0M $NaCO_3$ solution. The $NaCO_3$ solution was dropped into the reaction solution at flow rate of 10 ml·min^{-1} under continuous stirring until formation of a white deposit in the flask bottom. The solution was kept stirred while heated at 373 K for 2 h and then heated at 1073 K for 2 h to produce NSDC powder.

The $Li_{0.2}Ni_{0.7}Cu_{0.1}O$ (LNC-271) was synthesized by sol-gel reaction [10]. A stoichiometric amount of Li_2CO_3, $Cu(OH)_2$, and $NiCO_3·2Ni(OH)_2·4H_2O$ were mixed and dissolved in deionized water to produce 1.0M solution. Then, citric acid in the ratio of total cation to citric acid of 1:2 was added to the solution. The solution was stirred in a high speed to produce a homogeneous solution. The solution was stirred continuously and heated

at 373 K for 2 h, and then heated to 1073 K for 2 h to produce a black LNC-271 powder. All of the prepared materials were characterized by XRD (Bruker D8) to investigate their crystal structure and the available phases inside. A Le Bail refinement (in Rietica software, a free software edition) confirms the most possible crystal structure for the materials.

2.2. Single Cell of NSDC-L⎪NSDC⎪NSDC-L Preparation and Test with a Binary Liquid Mixture of Bioethanol-Water and Biodiesel-Water as Fuel

The biofuels used in this research were bioethanol 90% procured from bioethanol production unit, Bekonang, Central Java, Indonesia. Biodiesel Pertamina B20 was procured from PERTAMINA, Indonesia. The bioethanol 90% was diluted in deionized water (Aquabidestila sterile Aqua Pro Inject) to provide bioethanol 70%, 70 to 30 of bioethanol to water, respectively. Biodiesel B20 was mixed with deionized water at the ratio biodiesel-water as 70:30, and then named as biodiesel 70%.

The prepared NSDC was pressed in a disc with the diameter of 3 cm and thickness of 1 mm. The disc was sintered at 1073 K for 5 h. NSDC powder was mixed with LNC-271 powder at 1:1 ratio. The mixture was then added with α-terpineol under 1:1 ratio to form slurry of NSDC-L. The slurry was coated on both sides of NSDC disc by screen printing method, and then heated to 873 K for 2 h to produce a disc of NSDC-L⎪NSDC⎪NSDC-L. Both sides of a single cell were coated with silver paste and then a silver mesh (Nilaco Co.) was put on them and connected with a silver wire. The single cell along with silver mesh and silver wire as current collector was attached on an alumina tube by a ceramic glue. The scheme of single cell system and its measurement tools along with fueling system is depicted in Fig. 2. Single cell test was conducted with binary liquid of bioethanol-water 70:30 or bioethanol 70% and biodiesel 70% as fuels with the flow rate of 1–1.5 ml·min^{-1}. The fuels were analyzed by FTIR (Prestige-21 Shimadzu) and GC-MS (GC17A MS QP5000 Shimadzu) to identify the functional groups content and conduct molecular identification based on their retention peaks and molecular mass, respectively.

The fuel cell test was conducted at 673, 773, and 873 K. Loading resistance was tune by a potentiometer in the range between 100 and 1000 Ω. The I-V data were collected and used to calculate power density P (mW·cm^{-2}). The voltage was measured by a digital multimeter (Sanwa DMM CD8001 400 counts, millivolt unit), the current was measured by an Auto range digital multimeter (3999 counts constant 89, miliAmpere unit).
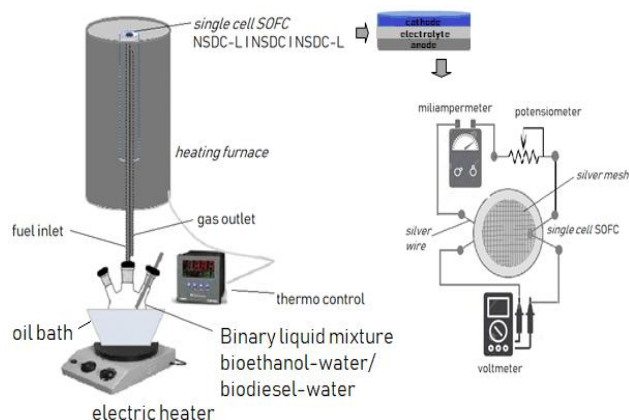
Fig. 2. Scheme of tools in a single cell NSDC-L⎪NSDC⎪NSDC-L test with the detail scheme of the single cell along with current collector and its measurement tools

3. Results and Discussion

The synthesized-SDC and NSDC have diffraction patterns as depicted in Fig. 3a. Le Bail plot of diffraction data for SDC and NSDC is shown in Figs. 3b and 3c, respectively. The diffraction patterns show that there is no peak between SDC and NSDC. It means that there are no peaks corresponding to NaCO$_3$ addition. The NaCO$_3$ seems to be an amorphous coating on SDC particles [15]. Le Bail refinement shows that NSDC consist of two phases of SDC and sodium oxide, Na$_2$O. It indicates that the carbonate was removed during heating treatment, and sodium was reacted with oxygen to form sodium oxide Na$_2$O. This is similar to our previous results regarding interaction between sodium carbonate with SDC [19]. The SDC phase was crystallized in a cubic structure with a space group of *Fm3m*, meanwhile the sodium oxide was also crystallized in a cubic structure *Fm3m*. The refinement results are listed in Table 1. Interaction between SDC with Na$_2$O changes the cell parameter from 5.423937(2) to 5.4370909(2) Å.

The diffraction pattern of NSDC-L is depicted in Fig. 4, compared with diffraction patterns of NSDC and LNC-271. The NSDC-L diffraction pattern shows characteristic peaks of NSDC and LNC-271. However, some minor peaks still appear at 2θ 34.36° and 36.70°. It indicates the presence of LiCO$_3$ as the remaining reactant even though after heating at 1073 K [21].

Physical characteristics of bioethanol 70% and biodiesel (B20) 70% are listed in Table 2. Meanwhile, the chemical characteristics are provided by functional group analysis in fuel as shown by FTIR spectrum (Fig. 5), and also gas chromatography analysis for carbon chain determination (Table 3).

**The refinement results of the synthesized SDC and NSDC compared
to SDC standard diffraction ICSD#28791 and Na₂O ICSD#60435**

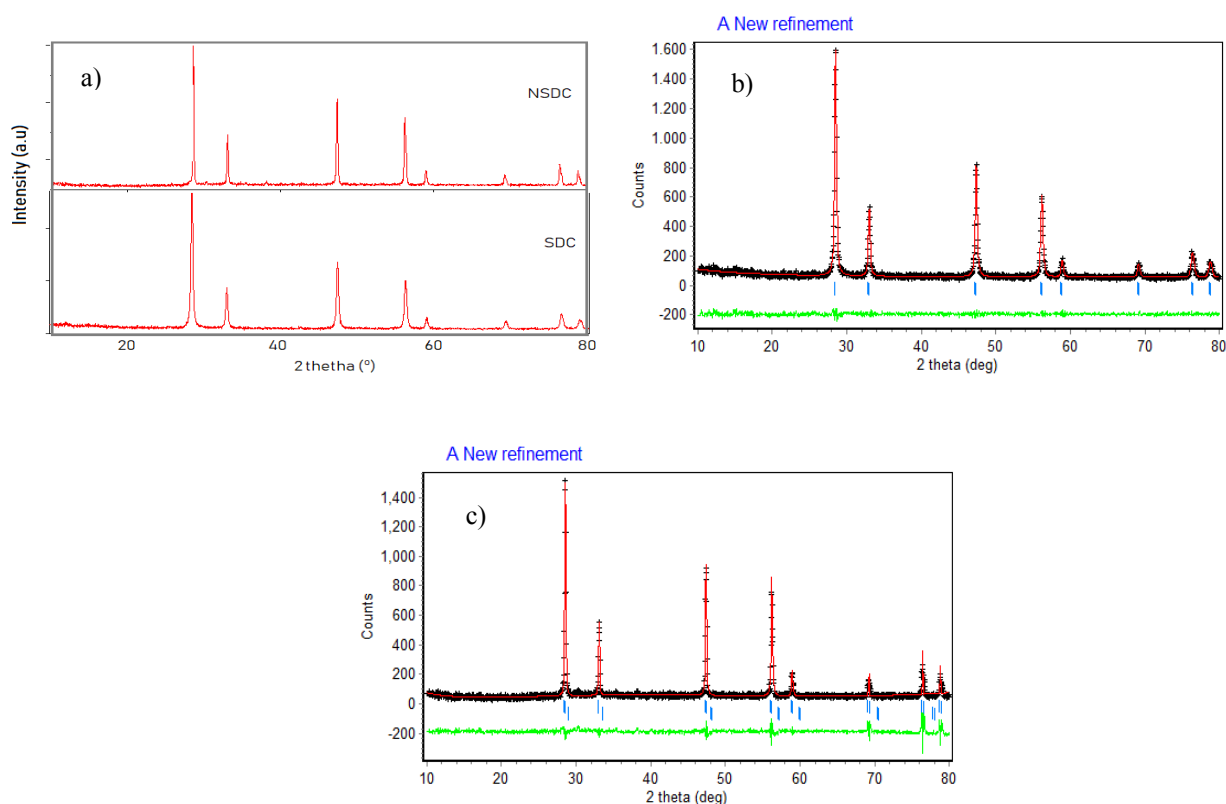| Cell parameters	SDC	NSDC	
Crystal structure	Cubic SDC	Cubic SDC	Cubic Na$_2$O
Space group	*Fm3m*	*Fm3m*	*Fm3m*
a, Å	5.423937(2)	5.4370909(2)	5.55(0)
b, Å	5.423937(2)	5.4370909(2)	5.55(0)
c, Å	5.423937(2)	5.4370909(2)	5.55(0)
Volume sel, Å^3	159.48	170.95	
Rp, %	7.828	3.87	
Rwp, %	7.926	3.80	

Fig. 3. Diffraction patterns of SDC and NSDC (a), the Le Bail plot of SDC (b), and the Le Bail plot of NSDC (c)

Functional groups analysis of bioethanol 70% and Biodiesel B20, as shown in Figs. 5 and 6, provides a broaden –OH stretch at 3363 cm^{-1}. Small peaks at 2975 and 2927 cm^{-1} indicate the presence of C–H stretch. Meanwhile, a peak at 1048 cm^{-1} is the peak of C–O stretch [22].

FT-IR spectra of biodiesel B20 as depicted in Fig. 6 shows a specific peak at 1169 cm^{-1} as the methyl ester –O–CH$_3$ peak, and a peak at 1745 cm^{-1} as a carbonyl C=O stretch [23]. The methylene CH$_2$– stretch appears at 2925 and 2853 cm^{-1}. Meanwhile, a methyl peak –CH$_3$ appears at 2956 cm^{-1} and two small peaks of methyl – at 1376 and 1462 cm^{-1}.
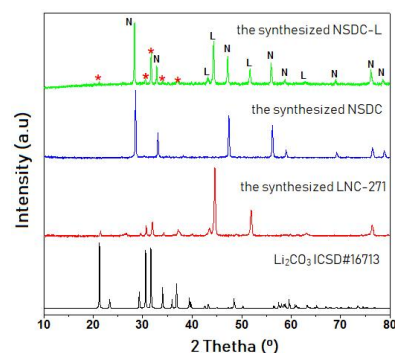

Fig. 4. Diffraction patterns of NSDC-L, LNC and NSDC; L refers to LNC, N refers to NSDC, and * sign refers to Li$_2$CO$_3$

GC-MS analysis of the fuels found that the bioethanol has a single peak retention time of 2.018 min, confirming a single ethanol composition, with the area of 100 %. Meanwhile, the biodiesel B20 GC-MS analysis shows a dominant retention time at 30.571 and 33.922 min, with the area of 22.8 and 18.3 %. MS analysis shows that those peaks are *n*-hexadecanediol and methyl oleat, with the molecular weight of 258 and 296 $g \cdot mol^{-1}$, respectively. Other peaks represent alkane and aromatic hydrocarbon with chain number of 9–27. The detail GC-MS results are depicted in Table 3.

During single cell test, the fuel vapor was flowed into anodic compartment, interacted with anode through four possible ways, which are partial oxidation (Eq. (1)),

gas-water shift or gas phase reaction (Eq. (2)) [24], and steam reforming (Eq. (3)) [25]. When SOFC is operated with direct internal reforming condition, the reforming reaction of fuel occurs simultaneously with electrochemical oxidation on anode and it will lead a complex anode reaction [14]. Ethanol also can undergo decomposition to H_2, CO, CH_4, and CO_2 (Eq. (4)) [7]. The internal gas reforming and the presence of H_2O as steam producer increase the possibility of H_2 forming, as described in Eq. (1), in which 6 moles of H_2 will be released in a steam reforming reaction. Within 373–573 K CO_2 and CH_4 gasses tend to form, while CO gas will be formed at above 673 K. All of the gas residues might increase H_2 production, that will also increase reaction in anode [26].

Table 2

Physical properties of bioethanol 70% and biodiesel 70%

Parameters	Fuels	
	Bioethanol	Biodiesel
Density, g/ml	0.89	0.85
Viscosity, cP	0.83	2.90
Color	Clear (no color)	Brownish yellow
Boiling point, K	357	423

Table 3

GC-MS analysis results for bioethanol and biodiesel B20

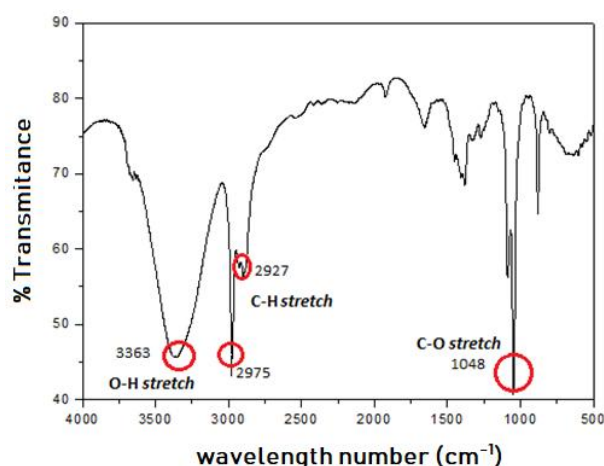| Fuels	Chemical formula	Area, %
Bioethanol	CH_3CH_2OH	100
Biodiesel (B20)	$C_{16}H_{34}O_2$	22.80
	$C_{19}H_{36}O_2$	18.30
	$C_{15}H_{32}, C_{14}H_{30}, C_{17}H_{36} C_{19}H_{40}, C_{16}H_{34}, C_{17}H_{36}, C_{13}H_{28,} C_{12}H_{26}, C_{18}H_{38}$	
	$C_9H_{20}, C_{10}H_{22}, C_{11}H_{24}$	3.18
	$\geq C_{19}H_{40}$	35.02
Total		100

Fig. 5. FT-IR spectra of bioethanol 70%

Fig. 6. FT-IR spectra of biodiesel B20

$$C_2H_5OH_{(l)} + \frac{1}{2}O_{2(g)} \leftrightarrow 3H_{2(g)} + CO_{(g)} \quad (1)$$

$$CO_{(g)} + H_2O_{(aq)} \leftrightarrow H_{2(g)} + CO_{2(g)} \quad (2)$$

$$C_2H_5OH_{(l)} + 3H_2O_{(aq)} \leftrightarrow 6H_{2(g)} + 2CO_{2(g)} \quad (3)$$
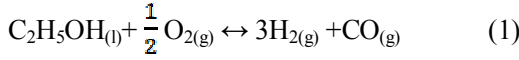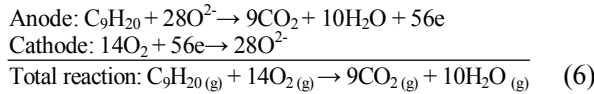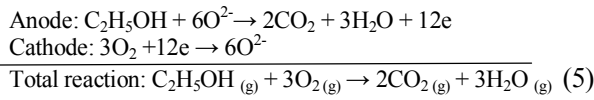
$$C_2H_5OH_{(l)} \leftrightarrow H_{2(g)} + CO_{(g)} + CH_{4(g)} \quad (4)$$
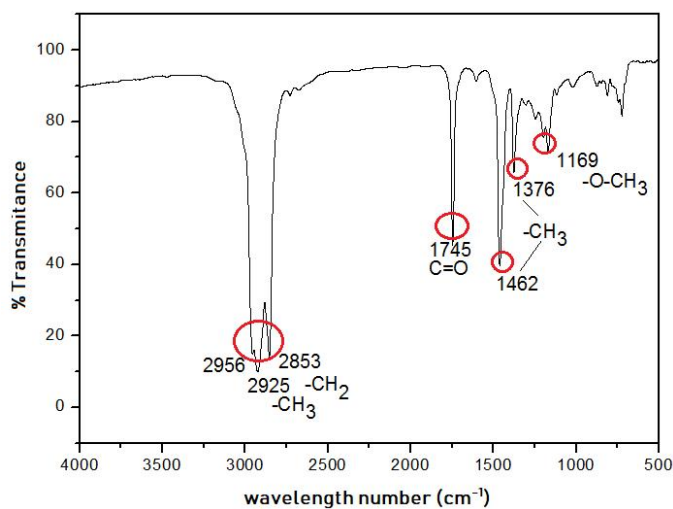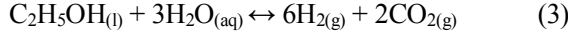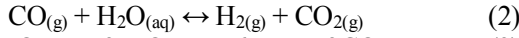
When bioethanol undergoes direct oxidation at anodic compartment (Eq. (5)), there are 12 electrons involved in the reaction. Besides a reaction between O^{2-} with H_2 produced from steam reforming according to Eq. (3), the gas-water shift may also provide more electrons production.

If biodiesel reaches anode compartment directly, the predicted reaction is represented by Eq. (6), based on the shortest carbon chain of C_9H_{20}.

$$\begin{aligned} \text{Anode: } &C_2H_5OH + 6O^{2-} \rightarrow 2CO_2 + 3H_2O + 12e \\ \text{Cathode: } &3O_2 + 12e \rightarrow 6O^{2-} \\ \hline \text{Total reaction: } &C_2H_5OH_{(g)} + 3O_{2(g)} \rightarrow 2CO_{2(g)} + 3H_2O_{(g)} \end{aligned} \quad (5)$$

$$\begin{aligned} \text{Anode: } &C_9H_{20} + 28O^{2-} \rightarrow 9CO_2 + 10H_2O + 56e \\ \text{Cathode: } &14O_2 + 56e \rightarrow 28O^{2-} \\ \hline \text{Total reaction: } &C_9H_{20(g)} + 14O_{2(g)} \rightarrow 9CO_{2(g)} + 10H_2O_{(g)} \end{aligned} \quad (6)$$

Fuel cell performance test that was conducted with bioethanol 70% and biodiesel 70% resulted in I-V curve and power density P as described in Figs. 7 and 8, respectively. Highest power density is observed at 673 K with the value of 2.984 mW·cm^{-2} for bioethanol fuel, with open circuit voltage of 1.439 V. Meanwhile, the maximum power density when the SOFC was operated with biodiesel 70% is 1.838 mW·cm^{-2} with open circuit voltage of 0.710 V (Fig. 8).

The data of single cell performance test with bioethanol 70% and biodiesel 70% as fuels are listed in Table 4.

The performance decreasing when the temperature is increased to 773 and 873 K, indicates high ohmic loss, probably caused by auto-reduction of Ce^{4+} to Ce^{3+}. Cerium ion is not stable at high temperature, and tends to undergo reduction reaction that may lead to short circuit between anode-cathode due to electron flows through electrolyte [27]. The power density produced in this research is still too low compared to another research that provided 148 mW·cm^{-2} at 853 K [10]. However, that was resulted by a 100–200 ml·min^{-1} rate of fuel flow. It is about 100 time faster than the fuel flow in this research, which is 1–1.5 ml·min^{-1}. When the fuel cell provides electricity at a very low fuel rate, it will also provide electricity at a higher fuel flow rate, therefore this result is still very promising, especially to extend the research to investigate the effect of fuel flow rate. Low degree of oxidation might also cause low fuel cell performance, as it occurs when a glycerol/O_2 biofuel for fuel cell only yields power density up to 1.21 mW·cm^{-2} [28]. A direct ethanol fuel cell using Pt75Ru15Ni10/C anode catalyst also achieved maximum power density only of 4 mW·cm^{-2} [29].

The decrease of fuel cell performance was also affected by electrochemical polarization, that might be caused by activation polarization, concentration polarization from anode and cathode, symbolized by η_a and η_b, respectively, as well as by the ohmic resistance R_Ω. Therefore, the total fuel cell operating voltage can be expressed as Eq. (7) [30].

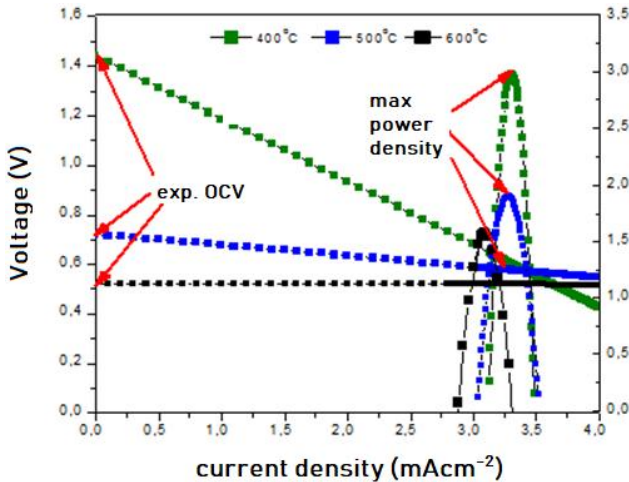$$V = V_{Nernst} - \eta_{total} = V_{Nernst} - \eta_a - \eta_c - IR_\Omega \quad (7)$$

Fig. 7. I-V curve and power density of NSDC-L│NSDC│NSDC-L with bioethanol 70% as fuel at different operational temperatures
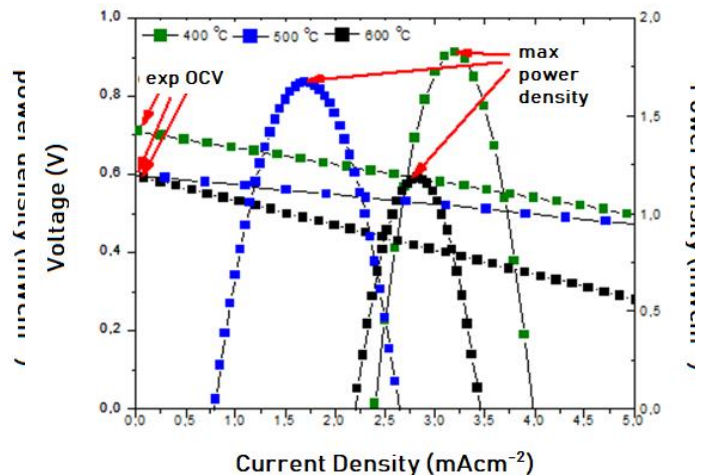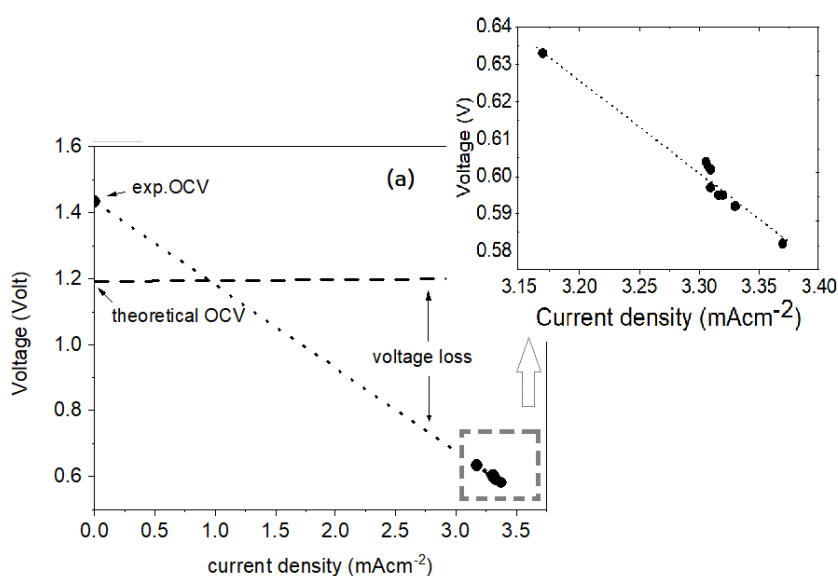

Fig. 8. I-V curve of NSDC-L│NSDC│NSDC-L with biodiesel 70% as fuel at different operational temperatures

**Open circuit voltage (OCV), and power density in a single cell NSDC-L│NSDC│NSDC-L
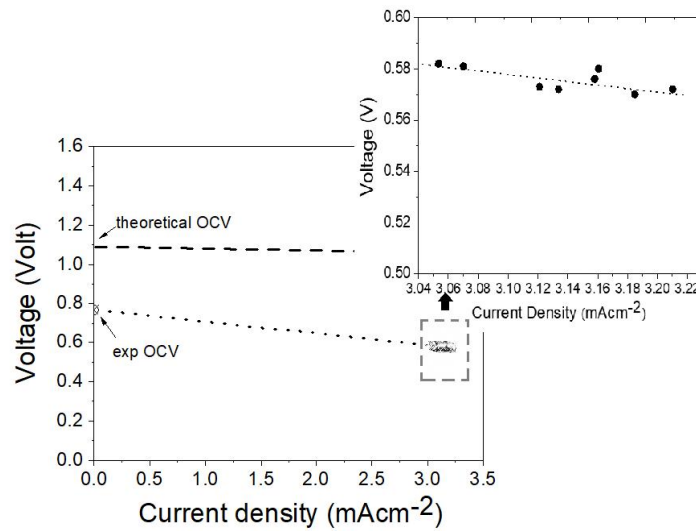with bioethanol 70% and biodiesel 70% as fuels at 673, 773 and 873 K**

Fuel	Operational temperature, K	Power density, mW·cm^{-2}	OCV, V
Bioethanol	673	2.984	1.439
	773	1.902	0.720
	873	1.597	0.515
Biodiesel	673	1.838	0.710
	773	1.658	0.600
	873	1.124	0.590

The polarization curves are depicted in Figs. 9 and 10. Ohmic loss is caused by internal resistance in the electrolyte or electrode materials. The internal resistance will reduce O^{2-} transfer rate from cathode to anode. In addition, fuel diffusion resistance also may affect the fuel cell performance. Molecular size might be a factor that causes different diffusion performance inside pores of electrode. It is hard for large molecules to diffuse into small size pores. This becomes the reason of the lower fuel cell performance when biodiesel was used as fuel. Polarization will cause fuel cell stability to decrease and allow potential loss, shown by the difference between theoretical and experimental OCV. Theoretical OCV is reversible potential calculated based on thermodynamics parameter value of each reaction. Calculation results compared to the experimental OCV are listed in Table 5. Experimental OCV of single cell with bioethanol 70% as fuel is 0.243 V which is higher than the theoretical OCV. It is probably caused by the fact that calculation for theoretical OCV is based only on Gibbs energy change of ethanol production involving CO_2 and steam H_2O, as written in Eq. (5). Meanwhile, the occurrence of gas reforming is possible at 673 K as described in Eqs. (1)-(4) to produce H_2, CO, CH_4, and CO_2. The presence of steam also can enrich H_2 production, therefore in anodic compartment, H_2 oxidation to H^+ may contribute to fuel cell performance to react with O^{2-} in cathode compartment. However, the increasing of electrical current load allows voltage drop as it is described in Fig. 9, due to the polarization increase in electrochemical system. Meanwhile, experimental OCV of single fuel cell with biodiesel 70% is 0.710 V, which is lower than theoretical OCV by 1.127 V. Large biodiesel molecules which mainly consist of $C_{16}H_{34}O_2$ might allow condensation due to gravitational effect. If the condensation occurs rapidly, less oxidation will take place in anode. Horizontal design of fuel cell can be considered to reduce gravitational effect in the future, because vertical design might not be reliable for a large molecule fuel. Addition of carrier gas such as N_2 may also can be considered to enhance the performance and durability of biogas-fueled SOFC [14].

**Fig. 9.** Polarization curve of single cell NSDC-L│NSDC│NSDC-L with bioethanol 70% as fuel

Fig. 10. Polarization curve of single cell NSDC-L│NSDC│NSDC-L
with biodiesel 70% as fuel

Fig. 11. Diffraction patterns of NSDC after being used in a single cell test with bioethanol 70% and biodiesel 70% as fuel, compared to the initial NSDC pattern. Small circles O refer to new peaks indicated as $LiCO_3$
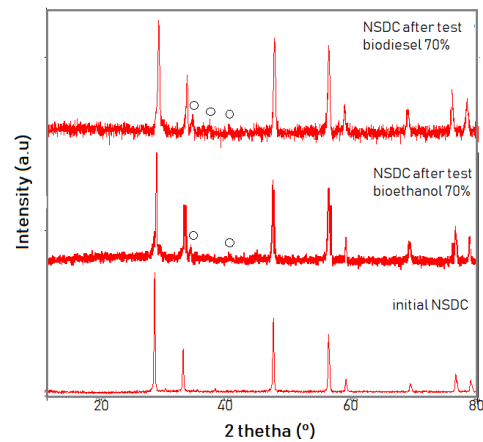
Analysis after single cell test was conducted to investigate stability of NSDC after being loaded with fuel under high temperature. XRD patterns after being loaded with bioethanol 70% and biodiesel 70% are depicted in Fig. 11, compared with the initial NSDC pattern. The patterns show new peaks at 2θ 35.38° and 36.78°, which are indicated as Li_2CO_3 characteristic peaks. It indicates Li migration from NSDC-L electrode to NSDC electrolyte during fuel cell operation.

Table 5

Open circuit values of single cell NSDC-L│NSDC│NSDC-L with bioethanol 70% and biodiesel 70%, and the theoretical OCV

Fuels	Theoretical OCV (volt)	Experimental OCV (volt)
Bioethanol 70 %	1.196	1.439
Biodiesel 70 %	1.127	0.710

4. Conclusions

A single fuel cell system NSDC-L│NSDC│NSDC-L can run with binary liquid mixture of bioethanol-water (70:30) and biodiesel-water (70:30) as fuel. At a very low flow rate of 1–1.5 ml·min^{-1}, the fuel cell shows power density of 2.984 mW·cm^{-2} at 673 K with bioethanol 70% as fuel, and 0.710 mW·cm^{-2} with biodiesel 70% as fuel. The values are still lower than in other researches on direct ethanol-SOFC due to some reasons, such as very low flow rate, vertical design used for the fuel cell system, and also voltage loss due to electrochemical system polarization.

Acknowledgements

References

[1] Alriksson B., Rose S., Van Z. *et al.*: Appl. Environ. Microbiol. J., 2009, **75**, 2366. https://doi.org/10.1128/AEM.02479-08

[2] Torres-Jimenez E., Svoljsal-Jerman M. *et al.*: Energ. Fuel, 2010, **24**, 2002. https://doi.org/10.1021/ef901158a

[3] Colella W., Jacobson M.,Golden D.: J. Power Sour., 2005, **150**, 150. https://doi.org/10.1016/j.jpowsour.2005.05.092

[4] Badwal S., Giddey S., Kulkarni A. *et al.*: Appl. Energ., 2015, **145**, 80. https://doi.org/10.1016/j.apenergy.2015.02.002

[5] Beuscher U., Cleghorn S., Johnson W.: Int. J. Energy Res., 2005, **29**, 1103. https://doi.org/10.1002/er.1142

[6] Dokmaingam P.: Eng. J., 2015, **19**, 1. https://doi.org/10.4186/ej.2015.19.2.1

[7] Nobrega S. *et al.*: J. Power Sources, 2012, **213**, 156, 2012. https://doi.org/10.1016/j.jpowsour.2012.03.104

[8] Kirubakaran R., Jain S., Nema R.: Sustain. Energy Rev., 2009, **13**, 2430. https://doi.org/10.1016/j.rser.2009.04.004

[9] Nobrega S., Fonseca F., Gelin P. *et al.*: Energy Procedia, 2012, **28**, 28. https://doi.org/10.1016/j.egypro.2012.08.037

[10] Qin H. *et al.*: Energy Environ. Sci., 2011, **4**, 1273. https://doi.org/10.1039/c0ee00420k

[11] Imran S., Raza R., Abbas G., Zhu B.: J. Fuel Cell Sci. Technol., 2011, **8**, 061014. https://doi.org/10.1115/1.4004475

[12] Hanna J., Lee W., Shi Y., Ghoniem A.: Prog. Energy Combust. Sci., 2014, **40**, 74. https://doi.org/10.1016/j.pecs.2013.10.001

[13] Helveg S., Lopez-Cartes C., Sehested J. *et al.*: Nature, 2004, **427**, 5. https://doi.org/10.1038/nature02278

[14] Lyu Z., Shi W., Han M.: Appl. Energ., 2018, **228**, 556. https://doi.org/10.1016/j.apenergy.2018.06.114

[15] Wang X., Ma Y., Raza R., Muhammed M., Zhu B.: Electrochem.Commun., 2008, **10**, 1617. https://doi.org/10.1016/j.elecom.2008.08.023

[16] Aslannejad H., Barelli L., Babaie A., Bozorgmehri S.: Appl. Energ., 2016, **177**, 179. https://doi.org/10.1016/j.apenergy.2016.05.127

[17] Steil M., Nobrega S., Georges S. *et al.*: Appl. Energ., 2017, **199**, 180. https://doi.org/10.1016/j.apenergy.2017.04.086

[18] Akdeniz Y., Timurkutluk B., Timurkutluk C.: Int. J. Hydrogen Energ., 2016, **41**, 10021. https://doi.org/10.1016/j.ijhydene.2016.03.169

[19] Rahmawati F., Syarif D., Paramita P., Heraldy E.: Adv. Mater. Res., 2014, **896**, 49. https://doi.org/10.4028/www.scientific.net/AMR.896.49

[20] Rahmawati F., Nuryanto A., Nugrahaningtyas K.: IOP Conf. Ser: Mater. Sci. Eng., 2016, **107**, 012035. https://doi.org/10.1088/1757-899X/107/1/012035

[21] Zhu W., Xia C., Ding D. *et al.*: Mater. Res. Bull., 2006, **41**, 2057. https://doi.org/10.1016/j.materresbull.2006.04.001

[22] Doroshenko I., Pogorelov V., Sablinskas V.: Dataset Pap. Chem., 2013, **2013**. https://doi.org/10.7167/2013/329406

[23] https://chem.libretexts.org/Ancillary_Materials/Reference/Reference_Tables/Spectroscopic_Parameters/Infrared_Spectroscopy_Absorption_Table

[24] Mattos L., Jacobs G., Davis B., Noronha F.: Chem. Rev., 2012, **112**, 4094. https://doi.org/10.1021/cr2000114

[25] Sukwattanajaroon V., Assabumrungrat S., Charojrochkul S. *et al.*: Bioethanol-Fuelled Solid Oxide Fuel Cell System for Electrical Power Generation [in]: Nayeripour M. (Ed.), Renewable Energy - Trends and Applications. IntechOpen 2011. https://doi.org/10.5772/22179

[26] Bion N., Epron F., Duprez D.: Bioethanol reforming for H2 production. A comparison with hydrocarbon reforming [in]: Spivey J., Dooley K. (Eds.), Catalysis v.22. Royal Society of Chemistry, Cambridge 2010, 1-55. https://doi.org/10.1039/9781847559630-00001

[27] Syahputra R., Rahmawati F., Prameswari A., Saktian R.: AIP Conf. Proceed., 2017, **1823**, 020061. https://doi.org/10.1063/1.4978134

[28] Arechederra R., Treu B., Minteer S.: J. Power Sources, 2007, **173**, 156. https://doi.org/10.1016/j.jpowsour.2007.08.012

[29] Ribadeneira E., Hoyos B.: J. Power Sources, 2008, **180**, 238. https://doi.org/10.1016/j.jpowsour.2008.01.084

[30] Yang T., Sezer H., Celik I. *et al.*: Int. J. Electrochem. Sci., 2017, **12**, 6801. https://doi.org/10.20964/2017.07.30

БІНАРНА РІДКА СУМІШ БІОЕТАНОЛ-ВОДА ТА БІОДИЗЕЛЬ-ВОДА ЯК ПАЛИВО ДЛЯ NSDC-L│NSDC│NSDC-L ЕТАНОЛ-ТВЕРДООКСИДНОГО ПАЛИВНОГО ЕЛЕМЕНТУ

Анотація. *Вивчено можливість використання бінарної рідкої суміші біоетанол-вода та біодизель-вода як палива для NSDC-L│NSDC│NSDC-L паливного елементу. Дослідження проводили за співвідношення біоетанол-вода і біодизель-вода 70:30, температури 673, 773, 873 К та швидкості витрати 1–1,5 мл·хв⁻¹. Визначено, що найвища питома потужність 2,984 мВт·см⁻² та 1,838 мВт·см⁻² для біоетанолу-води та біодизеля-води, відповідно, досягається за температури 673 К, що є багатообіцяючим результатом для паливного елементу з дуже низькою швидкістю витрати рідкого палива. Встановлено, що напруга розімкнутого ланцюга (НРЦ) паливного елемента з біоетаноло-водним паливом становить 1,439 В, що наближене до теоретичного зачення. НРЦ паливного елемента з біоди-зель-водним паливом становить 0,710 В, що нижче теоретич-ного значення. Показано, що явище поляризації залишається проблемою, яка спричиняє втрату напруги під час випробу-вання на паливному елементі.*

Ключові слова: *бінарна рідка суміш, паливо, твердо-ксидний паливний елемент, NSDC.*